Research Article

KNAT7 positively regulates xylan biosynthesis by directly activating *IRX9* expression in *Arabidopsis*

Running Title: KNAT7 positively regulates xylan biosynthesis

Jun-Bo He[1, 2], Xian-Hai Zhao[1, 2], Ping-Zhou Du[3†], Wei Zeng[4], Cherie T Beahan[4], Yu-Qi Wang[3, 5], Hui-Ling Li[1, 2, 6], Antony Bacic[4], Ai-Min Wu[1, 2*]

[1]. State Key Laboratory for Conservation and Utilization of Subtropical Agro-bioresources, South China Agricultural University, Guangzhou 510642, China

[2]. Guangdong Key Laboratory for Innovative Development and Utilization of Forest Plant Germplasm, College of Forestry and Landscape Architecture, South China Agricultural University, Guangzhou 510642, China

[3]. College of Life Sciences, South China Agricultural University, Guangzhou 510642, China

[4]. ARC Centre of Excellence in Plant Cell Walls, School of BioSciences, The University of Melbourne, Parkville VIC 3010, Australia

[5]. Boyce Thompson Institute for Plant Research, Ithaca, NY 14853, USA

[6]. Provincial Key Laboratory of Agrobiology, Jiangsu Academy of Agricultural Sciences, Nanjing 210014, China

[†] Current address: Key Laboratory of Cell Proliferation and Regulation Biology of Ministry of Education, College of Life Science, Beijing Normal University, Beijing 100875, China

* **Correspondence:** Ai-Min Wu (wuaimin@scau.edu.cn)

Edited by: Vincent Bulone, AlbaNova University Centre, Sweden

This is the author manuscript accepted for publication and has undergone full peer review but has not been through the copyediting, typesetting, pagination and proofreading process, which may lead to differences between this version and the Version of Record. Please cite this article as doi: 10.1111/jipb.12638

Abstract

Xylan is the major plant hemicellulosic polysaccharide in the secondary cell wall. The transcription factor KNOTTED-LIKE HOMEOBOX OF ARABIDOPSIS THALIANA 7 (KNAT7) regulates secondary cell wall biosynthesis, but its exact role in regulating xylan biosynthesis remains unclear. Using transactivation analyses, we demonstrate that KNAT7 activates the promoters of the xylan biosynthetic genes, *IRREGULAR XYLEM 9* (*IRX9*), *IRX10*, *IRREGULAR XYLEM 14-LIKE* (*IRX14L*), and *FRAGILE FIBER 8* (*FRA8*). The *knat7* T-DNA insertion mutants have thinner vessel element walls and xylary fibers, and thicker interfascicular fiber walls in inflorescence stems, relative to wild-type (WT). *KNAT7* overexpression plants exhibited opposite effects. Glycosyl linkage and sugar composition analyses revealed lower xylan levels in *knat7* inflorescence stems, relative to WT; a finding supported by labeling of inflorescence walls with xylan-specific antibodies. The *knat7* loss-of-function mutants had lower transcript levels of the xylan biosynthetic genes *IR*X9, *IRX10*, and *FRA8*, whereas *KNAT7* overexpression plants had higher mRNA levels for *IRX9*, *IRX10*, *IRX14L*, and *FRA8*. Electrophoretic mobility shift assays indicated that KNAT7 binds to the *IRX9* promoter. These results support the hypothesis that KNAT7 positively regulates xylan biosynthesis.

INTRODUCTION

The secondary cell wall consists primarily of cellulose, hemicellulose, and lignin in approx. equal proportions. Xylan is the major hemicellulose component in secondary walls of most dicots and monocots, and consists of a linear backbone of β-(1-4)-linked D-xylosyl (Xyl) residues and α-linked (+/- OMe (methyl)) glucuronic acid (GlcA) side branches (Scheible and Pauly 2004; Zhang and Zhou 2011; Pauly et al. 2013). Additionally, a distinct tetrasaccharide sequence, 4-β-D-xylose-(1-3)-α-L-rhamnose-(1-2)-α-D-galacturonic acid-(1-4)-D-xylose is present at the reducing end of the xylan backbone, in gymnosperms and dicots (Johansson and Samuelson 1977; Andersson et al. 1983; Peña et al. 2007).

In *Arabidopsis thaliana*, *IRREGULAR XYLEM 9* (*IRX9*), *IRX10*, *IRREGULAR XYLEM 9-LIKE* (*IRX9L*), *IRX10*, *IRX10L*, *IRX14,* and *IRX14L* are involved in xylan backbone extension, whereas *FRAGILE FIBER 8* (*FRA8*), *FRA8 HOMOLOG* (*F8H*), *IRX8*, and *PARVUS* are associated with the biosynthesis of the xylan reducing end tetrasaccharide (Brown et al. 2007, 2009; Lee et al. 2007a, 2007b, 2009, 2012c; Wu et al. 2009, 2010; Jensen et al. 2014; Urbanowicz et al. 2014). Addition of GlcA side chains, in the *Arabidopsis* xylan, is mediated by GLUCURONIC ACID SUBSTITUTION OF XYLAN 1 (GUX1), GUX2, and GUX3 (Mortimer et al. 2010; Lee et al. 2012a; Bromley et al. 2013) and approx. 60% of the GlcA side chains are methylated, at O-4, a process catalyzed by GLUCURONOXYLAN METHYLTRANSFERASE 1 (GXM1), GXM2, and GXM3 (Lee et al. 2012b; Urbanowicz et al. 2012). Four *REDUCED WALL ACETYLATION* (*RWA*) genes and *ESKIMO 1* (*ESK1*) are involved in acetylation of the xylan main chain, at O-2 and O-3 (Lee et al. 2011; Xiong et al. 2013; Yuan et al. 2013). *IRX15* and *IRX15L* may be involved in xylan biosynthesis, but their precise functions remain unclear (Brown et al. 2011; Jensen et al. 2011). Recent studies revealed that the cytosolic UDP-Xylose synthases (UXSs) for UDP-Xylose substrate biosynthesis and UDP-Xylose transporters (UXTs) for UDP-Xylose transport from cytosol to Golgi lumen were also involved in xylan backbone elongation (Kuang et al., 2016; Zhao et al., 2017).

Xylem differentiation provides a model system for cell wall studies; this differentiation forms conductive vessel elements and supportive fiber cells. After xylem cell differentiation, secondary wall biosynthesis commences, involving deposition of cellulose, hemicellulose, and lignin, and results in strengthened walls. Many classes of transcription factors (TFs) function in xylem differentiation, including AUXIN/INDOLEACETIC ACID (Aux/IAA), AUXINRESPONSE FACTOR (ARF), class III HOMEODOMAIN LEUCINE-ZIPPER (HD-ZIP III), and the basic helix–loop–helix (bHLH) TFs TARGETS OF MONOPTEROS5 (TMO5) and LONESOME HIGHWAY (LHW) (Ohtani et al. 2016).

A systematic analysis of high-spatial-resolution gene expression datasets and yeast one-hybrid screens indicated that the E2Fc TF, which is upstream of VASCULAR RELATED NAC-DOMAIN PROTEIN6 (VND6) and VND7, might be the top-level master regulator of secondary wall biosynthesis (Taylor-Teeples et al. 2015). NAC (NAM, ATAF1/2, and CUC2) TFs are also master regulators of secondary wall biosynthesis. Of these, VND1–VND7 regulate secondary wall biosynthesis in vessels (Kubo et al. 2005; Yamaguchi et al. 2008; Zhou et al. 2014), whereas NAC SECONDARY WALL THICKENING PROMOTING FACTOR1 (NST1), NST2 and NST3/SECONDARY WALL-ASSOCIATED NAC DOMAIN PROTEIN1 (SND1) control this process in fibers (Zhong et al. 2006; Mitsuda et al. 2007; Zhong and Ye 2015).

Two MYB TFs, MYB46 and MYB83, act as second-level regulators (Zhong et al. 2007; Ko et al. 2009; McCarthy et al. 2009) to activate a battery of downstream TFs, including SND2, SND3, MYB20, MYB42, MYB43, MYB52, MYB54, MYB58, MYB63, MYB69, MYB85, MYB103, and KNAT7 (Zhong et al. 2008; Zhong and Ye 2012; Taylor-Teeples et al. 2015), which consequently regulate the biosynthesis of cellulose, xylan, and lignin (Zhong and Ye 2014). Regulation of the lignin monolignol biosynthetic pathway genes by MYB TFs has been well characterized since most of these genes contain AC cis-elements in their promoters (Hatton et al. 1995; Boerjan et al. 2003; Zhong et al. 2010a), but the regulation of xylan synthesis remains unclear.

KNAT7 is one of eight *Arabidopsis KNOTTED1-LIKE HOMEBOX* (*KNOX*) genes, and it has

been postulated to play a role regulating secondary cell wall biosynthesis (Li et al. 2012). *KNAT7* expression increases in concert with secondary cell wall development in the *Arabidopsis* inflorescence stem (Ehlting et al. 2005; Zhong et al. 2008); its dominant repression causes a reduction in secondary cell wall thickening in both vessel elements and fibers (Zhong et al. 2008). The *knat7* T-DNA insertion mutants exhibit inward collapsed vessel elements (*irx* phenotype) and lower levels of xylose in inflorescence stems compared to wild-type (WT) (Brown et al. 2005). These *knat7* mutants have thinner vessel element cell walls, in inflorescence stems, a reduced xylem:phloem ratio in secondary thickened hypocotyls and abnormally thick radial cell walls in seed coat epidermal cells (Romano et al. 2012). Furthermore, in virus-induced *Nicotiana benthamiana* (*Nb*) *KNAT7*-silenced and *NbKNAT7* RNAi plants, fiber cell walls are thinner and transcript levels of some cellulose, xylan, and lignin biosynthetic genes are reduced, whereas the opposite is observed in *NbKNAT7* overexpression plants (Pandey et al. 2016). Dominant repression of the *KNAT7* homolog, *Gossypium hirsutum KNOTTED1-LIKE* (*GhKNL1*) results in significantly shorter fibers and thinner fiber cell walls, relative to WT cotton (Gong et al. 2014).

KNAT7 acts as a transcriptional repressor that negatively regulates secondary cell wall biosynthesis (Li et al. 2011, 2012; Bhargava et al. 2013; Liu et al. 2014). It represses VP16-activated transcription of the *β-GLUCURONIDASE* (*GUS*) reporter gene (Li et al. 2011) and the expression of the *GUS* reporter gene driven by −46 base pair (bp) *Cauliflower mosaic virus* (CaMV) *35S* promoter (Bhargava et al. 2013). The *knat7* mutants have thicker fiber cell walls, higher lignin content and higher expression levels of many secondary cell wall biosynthetic genes in inflorescence stems, whereas *KNAT7* overexpression (*KNAT7-OE*) leads to thinner cell walls in interfascicular fibers (Li et al. 2012). KNAT7 interacts with BEL1-LIKE HOMEODOMAIN 6 (BLH6) and the KNAT7–BLH6 protein complex operates as a repression module in secondary wall formation by directly repressing the expression of *INTERFASCICULAR FIBERLESS 1* (*IFL1*) (Liu et al. 2014). *IFL1* loss-of-function mutants have abnormal fibers and vessel elements in inflorescence stems (Zhong and Ye 1999).

However, one study showed that *blh6* mutants contain less lignin relative to WT (Cassan-Wang et al. 2013).

Although previous work reported that KNAT7 regulates secondary cell wall biosynthesis, a detailed analysis focused on hemicellulosic xylan has not been conducted. Here, we report that KNAT7 activates the promoters of *IRX9*, *IRX10*, *IRX14L*, and *FRA8*. Xylan content and expression levels of *IRX9*, *IRX10*, and *FRA8* decrease in *knat7* mutants, whereas expression levels of *IRX9*, *IRX10*, *IRX14L*, and *FRA8* increase in *KNAT7*-OE plants. In addition, we establish that KNAT7 can bind to the *IRX9* promoter. These results support the hypothesis that KNAT7 positively regulates xylan backbone biosynthesis and directly induces *IRX9* expression.

RESULTS

KNAT7 activates the promoters of *IRX9*, *IRX10*, *IRX14L*, and *FRA8*

To screen TFs regulating xylan biosynthesis, in *Arabidopsis*, we conducted transactivation analyses of TFs that regulate secondary cell wall biosynthesis. We engineered effector constructs by fusing the TF genes downstream of the CaMV *35S* promoter, and engineered reporter constructs by fusing the promoters of *IRX9*, *IRX9L*, *IRX10*, *IRX10L*, *IRX14*, *IRX14L*, *FRA8*, and *F8H* in front of the *FIREFLY LUCIFERASE* (*FLUC*) reporter gene (Figure 1A). The reference construct contained the *RENILLA LUCIFERASE* (*RLUC*) reporter gene downstream of the CaMV *35S* promoter (Figure 1A). The promoter lengths used for *IRX9*, *IRX9L*, *IRX10*, *IRX10L*, *IRX14*, *IRX14L*, *FRA8*, and *F8H* were 2,045, 1,432, 825, 2,514, 2,855, 541, 2,501, and 2,502 bp, respectively, upstream from the start codon, based on distances from upstream genes. The effector, reporter, and reference constructs were co-transfected into *Arabidopsis* leaf protoplasts for transactivation analyses. These assays indicated that KNAT7 significantly induced expression of the *FLUC* reporter gene driven by the promoters of *IRX9*, *IRX10*, *IRX14L*, and *FRA8,* but not *IRX9L*, *IRX10L*, *IRX14*, and *F8H* (Figure 1B).

Xylan content analysis of *knat7* mutants

Based on the finding that KNAT7 activates the promoters of the major xylan backbone biosynthetic genes *IRX9*, *IRX10*, *IRX14L*, and *FRA8* (Figure 1B), we next investigated whether *KNAT7* affects xylan content in *Arabidopsis*. To this end, we identified a T-DNA insertion mutant allele of *KNAT7* (SALK_110899) that exhibited a similar phenotype to other independent T-DNA insertion mutant alleles of *KNAT7* (Li et al. 2012). The full transcript of *KNAT7* was undetectable in plants homozygous for the *knat7* allele, based on reverse transcription-polymerase chain reaction (RT-PCR) assays (Figure 2A).

Xylan content of the alcohol-insoluble residue (AIR) fraction of 7-week-old *knat7* mutant lower inflorescence stems was analyzed by enzyme linked immunosorbent assay (ELISA) with the monoclonal LM10 (rat immunoglobulin class IgG2c) and LM11 (class IgM) antibodies that specifically recognize xylan (McCartney et al. 2005). Here, we determined that the xylan content was decreased by 14% in *knat7* relative to WT plants (Figure 2B). Non-cellulosic monosaccharide composition was also analyzed; Xyl and GlcA content was decreased in *knat7* mutants compared to WT (Figure 2C). Glycosyl linkage analysis indicated that the xylan content in mature inflorescence stems from the *knat7* mutants was decreased by 17% relative to WT plants (Table 1). To further verify the defect in xylan content in *knat7* mutant plants, compared to WT, ^{1}H-NMR spectra of the purified xylo-oligosaccharides obtained from the AIR fractions showed that mutants had more (4-OMe) GlcA side chains (Figure 2D). Therefore, *knat7* mutants contained less xylan but had a higher (4-OMe) GlcA side chain content.

KNAT7 regulates secondary cell wall formation

A previous study reported that the *knat7* T-DNA insertion mutants (SALK_002098) had thicker interfascicular and xylary fiber cell walls, but thinner vessel element cell walls in inflorescence stems, and there was a striking decrease in the thickness of secondary walls in interfascicular fibers of

KNAT7-OE plants compared to WT (Li et al. 2012), which is seemingly at odds with our observation that *knat7* mutants contained less xylan (Figure 2; Table 1). To elucidate in more detail how KNAT7 regulates secondary cell wall biosynthesis, we examined cross-sections taken from the base of inflorescence stems of 6-week-old *knat7* mutants and *KNAT7*-OE plants. The full-length coding sequence of *KNAT7* was fused downstream of the CaMV*35S* promoter in a binary vector and the expression constructs were transformed into WT plants and *knat7* mutants to generate *KNAT7*-OE plants and conduct complementation experiments. *KNAT7* expression levels and anatomical phenotypes of the transgenic plants were assayed in the 6-week-old T_2 generation. RT-PCR indicated that *KNAT7* was over-expressed in *KNAT7*-OE plants (Figure 3A) but its expression was similar to WT in *35S*:*KNAT7*/*knat7* plants (Figure 3B).

Vessel element, xylary fiber and interfascicular fiber cell wall thicknesses were measured under high magnification light microscopy on toluidine blue stained thin sections. The vessel elements in inflorescence stems of *knat7* mutants exhibited an *irx* type phenotype, which could be rescued by *KNAT7* expression driven by CaMV*35S* (Figure 3C). The *knat7* mutants had thinner vessel element and xylary fiber secondary cell walls in inflorescence stems than WT plants, whereas *KNAT7*-OE plants showed the opposite phenotype (Figure 3C; Table 2). There was a >25% increase in cell wall thickness of interfascicular fibers in the *knat7* mutants and a decrease in thickness in *KNAT7*-OE plants compared to WT (Figure 3C; Table 2).

KNAT7 regulates expression of *IRX9*, *IRX10*, *IRX14L*, and *FRA8*

We next investigated the expression of *IRX9*, *IRX9L*, *IRX10*, *IRX10L*, *IRX14*, *IRX14L*, *FRA8*, and *F8H* in the lower half of inflorescence stems of 6-week-old *knat7* mutant and *KNAT7*-OE plants by quantitative real-time PCR (qRT-PCR). Gene expression of *IRX9*, *IRX10*, and *FRA8* was significantly down-regulated in the *knat7* mutant, but unchanged for the other genes tested (Figure 4A). *KNAT7*-OE plants showed increased expression of *IRX9*, *IRX10*, *IRX14L*, and *FRA8* (Figure 4B).

KNAT7 binds to the *IRX9* promoter

KNAT7 activates expression of the *FLUC* reporter gene driven by the *IRX9* promoter (Figure 1B), and regulates *IRX9* expression, *in vivo* (Figure 4), leading us to examine whether it binds to the *IRX9* promoter. Unfortunately, using the electrophoretic mobility shift assay, the protein–probe complexes and long free probes could not be effectively separated by electrophoresis. Consequently, we performed transactivation analyses with reporter constructs containing 5′ deletions of the *IRX9* promoter to identify the possible KNAT7 binding region. These assays indicated that the DNA fragment located between −492 and −1 bp relative to the start codon was effective for activation by KNAT7 (Figure 5A). There appears to be a KNAT7 binding element between −492 and −1,041 bp, which causes a significant decrease in activation between the −1,041 to −1 bp and the −492 to −1 bp fragments. Further 5′ deletion of approximately 100 bp from the −492 bp position indicted that the −209 to −1 bp fragment was activated by KNAT7, even though the level of activation was much lower than the −325 to −1 bp fragment. However, the −116 to −1 bp fragment was not activated by KNAT7 (Figure 5A). These results suggested that the −209 to −117 bp fragment contained the KNAT7 binding element.

Next, we performed EMSA using biotin-labeled −209 to −157 bp and −169 to −117 bp fragments of the *IRX9* promoter and recombinant GLUTATHIONE S-TRANSFERASE (GST)-KNAT7 fusion protein. However, no mobility shift was observed (Figure 5B). Based upon the transactivation analyses we concluded that the −209 to −1 bp fragment contained most of the KNAT7 binding element, whereas the −325 to −1 bp fragment contained the entire element. We then conducted EMSA with the biotin-labeled −236 to −184 bp *IRX9* promoter fragment and here we observed that the recombinant KNAT7 protein bound to the *IRX9* promoter fragment and caused a mobility shift (Figure 5C). This mobility shift gradually diminished as the concentration of competing unlabeled *IRX9* promoter fragment increased, and was not seen when the *IRX9* promoter fragment was

incubated with GST alone. This indicated that the direct binding of KNAT7 to the *IRX9* promoter was specific.

DISCUSSION

Despite the importance of xylans as components of the secondary cell wall, the transcriptional regulation of xylan biosynthesis is less fully understood than that of cellulose or lignin. In this study, we show that KNAT7 activates the expression of four xylan biosynthetic genes, *IRX9*, *IRX10*, *IRX14L*, and *FRA8* based on the following lines of evidence. First, KNAT7 activates expression, in leaf protoplasts, of the *FLUC* reporter gene driven by the *IRX9*, *IRX10*, *IRX14-L*, or *FRA8* promoters (Figure 1B). Second, *IRX9*, *IRX10*, and *FRA8* expression is significantly reduced in *knat7* mutants (Figure 4A). Third, *IRX9*, *IRX10*, *IRX14L*, and *FRA8* expression is induced by over-expression of *KNAT7* (Figure 4B). Given that *IRX14-L* expression was not reduced in *knat7* mutants, we can hypothesize that it is activated by other TFs (Figure 3B). However, previous studies on *knat7* mutants showed that *knat7* mutants also have increased *IRX9* and *FRA8* expression, while levels of *IRX10* are similar to WT (Li et al. 2012). Another study showed that *knat7* mutants expressed more *IRX9*, almost equal *IRX9L* and *FRA8*, and less *IRX10* relative to WT plants (Liu et al. 2014). MYB46 is known to directly activate *IRX14L* expression (Zhong and Ye 2012) and positively regulate the expression of *IRX9* and *FRA8* (Zhong et al. 2007; Ko et al. 2009). Transactivation analyses for MYB46 (Figure S1) are in accordance with these earlier studies and, hence, consistent with our transactivation analyses of KNAT7.

Based on our EMSA, KNAT7 appears to induce *IRX9* expression by binding directly to the *IRX9* promoter (Figure 5C). This is consistent with *KNAT7* and *IRX9* expression patterns; both are expressed in stem and root cells undergoing secondary wall formation (Peña et al. 2007; Zhong et al. 2008; Liu et al. 2014), indicating they likely function in these same cell types. As KNAT7 directly induces *IRX9* expression, our findings suggest that KNAT7 is a transcriptional activator, rather than a

repressor, as reported by others (Li et al. 2011; Bhargava et al. 2013). We propose that binding of the GD-KNAT7 fusion protein to the *Gal4* sequence likely hinders LD-PV6 fusion protein binding to the adjacent *LexA* sequence. This results in a decrease in *GUS* reporter gene expression in transactivation analyses (Li et al. 2011), since PV6 is a known strong transactivation domain (Zuo et al. 2000). If the transactivation activity of KNAT7 is weaker than the −46 bp CaMV *35S* promoter, the binding of the GD-KNAT7 fusion protein to the *Gal4* sequence may also affect the function of the adjacent −46 bp CaMV*35S* promoter, causing a decrease in *GUS* reporter gene expression in these analyses (Bhargava et al. 2013).

Our results are in conflict with the proposal that KNAT7 negatively regulates secondary cell wall biosynthesis as a transcriptional repressor (Li et al. 2011, 2012). Moreover, the expression of *KNAT7* is directly activated by the transcriptional activators SND1 and MYB46, which are positive master regulators of secondary cell wall biosynthesis, and the phenotype of KNAT7 dominant repression mutants is similar to both SND1 and MYB46 dominant repression mutants, namely reduced secondary wall thickness in both vessel elements and fibers in inflorescence stems (Zhong et al. 2006, 2007, 2008; Zhong and Ye 2012). Therefore, we conclude that KNAT7 is unlikely to be a transcriptional repressor.

Based on our studies, KNAT7 positively regulates xylan biosynthesis. In support of this hypothesis, *knat7* mutants had decreased xylan contents (Figures 2B−D; Table 1), and some xylan biosynthetic genes (*IRX9*, *IRX10*, and *FRA8*) had reduced expression in *KNAT7* loss-of-function mutants, and other genes (*IRX9*, *IRX10*, *IRX14L*, and *FRA8*) had enhanced expression in *KNAT7*-OE lines compared to WT plants (Figure 4). Furthermore, this KNAT7 function is consistent with findings from studies involving NbKNAT7, as xylan content decreased in virus-induced *NbKNAT7*-silenced and *NbKNAT7* RNAi plants, and increased in the *NbKNAT7* over-expression plants (Pandey et al. 2016). In addition, previous studies have indicated that an intact xylan synthase complex (XSC), comprised of IRX9, IRX10, and IRX14, is responsible for xylan biosynthesis (Zeng et al. 2016).

Although there were only minor effects on *IRX10* and *IRX14* expression, *knat7* and *KNAT7*-OE strongly affected *IRX9* expression (Figure 4), suggesting that control over xylan biosynthesis might occur through modulation of IRX9 levels in the XSC.

Contrary to KNAT7 positively regulating xylan biosynthesis, we determined that *knat7* mutants contain a greater amount of lignin compared to WT (Figure S2; the lignin content was measured by pyrolysis gas chromatography-mass spectrometry). It has been reported that *knat7* mutants contain more lignin, and consistent with this finding, a suite of lignin biosynthetic genes involved in secondary wall deposition is up-regulated in *knat7* mutants (Li et al. 2012, Liu et al. 2014). Consequently, KNAT7 could negatively regulate lignin biosynthesis.

In our study, *knat7* mutants had thinner vessel element and xylary fiber cell walls, but thicker interfascicular fiber cell walls, in inflorescence stems compared to WT, and *KNAT7*-OE plants exhibited the opposite phenotype (Figure 3; Table 2). These findings are not in complete concordance with the earlier study of Li et al. (2012). Taken together with the observation that *knat7* seed coat epidermal cells have abnormally thick radial cell walls (Romano et al. 2012), it would appear that KNAT7 does not simply activate or repress every component of the secondary wall equally. Rather, it differentially induces or represses the deposition of various components in specific cell types. Recently, the E2Fc TF (Taylor-Teeples et al. 2015), which can bind to promoters of VND6, VND7 and MYB46, was shown to be a positive activator of secondary cell wall biosynthesis, whereas it is also a negative regulator of endo-reduplication (del-Pozo et al. 2002, 2006). Thus, E2Fc functions in different transcriptional complexes to have seemingly opposite effects. It is, therefore, possible that KNAT7 functions in a similar manner: either as an activator or repressor, depending upon the composition of the complex in different tissue/cell types.

We have demonstrated that KNAT7 directly activates *IRX*9 expression and also activates *IRX10*, *IRX14L*, and *FRA8* expression. These findings enrich our understanding of the transcriptional network involved in the regulation of xylan biosynthesis (Figure 6). In this network, VND6, VND7, SND1,

NST1, and NST2, the master regulators of secondary wall biosynthesis, directly activate the expression of TF genes *MYB46, MYB83*, and *KNAT7* and xylan biosynthetic genes *IRX10*, *IRX14L*, and *PARVUS* (Zhong et al. 2008, 2010b; McCarthy et al. 2009). MYB46 and MYB83, the second-level regulators, directly activate the expression of *KNAT7* and the xylan biosynthetic gene *IRX14L* (Zhong et al. 2012). KNAT7 acts as the master downstream TF.

MATERIALS AND METHODS

Plant material and growth conditions

Arabidopsis thaliana (L.) Heynh ecotype Columbia-0 (Col-0) was used as the WT plant, and for construction of the mutants and transgenic lines. Plants were grown at 22°C with a 16/8 h (light/dark) photoperiod at approximately 120 μmol m^{-2} sec^{-1} light on soil. The T-DNA insertion mutant allele of *KNAT7*, SALK_110899, designated *knat7*, was identified using the SIGnal database (http://signal.salk.edu/) and seeds were obtained from the *Arabidopsi*s Biological Resources Center (ABRC, Columbus, OH, USA). *KNAT7* gene-specific primers (5′-AAGCCTGATATGCCCTTACGC-3′, 5′-GCTTCAAAGAACAGCTGCAAC-3′) and the T-DNA-specific primer LBb1.3 (5′-ATTTTGCCGATTTCGGAAC-3′) were used for PCR genotyping.

WT and *knat7* plants were used for transformation by *Agrobacterium tumefaciens* GV3101 using the floral dip method (Clough and Bent 1998). Transgenic plants were selected by Basta and confirmed by RT-PCR. Phenotypes of transgenic plants were examined in the T1 and T2 generations and at least two lines with similar phenotypes were obtained and results were representative.

Vector construction

The coding sequences of TF genes were cloned into the pUGW2 vector to generate effector constructs. The promoters of the xylan backbone biosynthetic genes were cloned into the pUGW35 vector to produce reporter constructs. For the *KNAT7*-OE construct, the coding sequence of *KNAT7* was cloned

into the pEarleyGate100 vector. The 249 bp terminal coding sequence of *KNAT7* was cloned into the pGEX-4T-2 vector downstream of the *GST* coding sequence to construct the GST-KNAT7 expression construct. The cloning primers were shown in Table S1. The vectors above were constructed using Gateway Technology (Walhout et al. 2000).

Transactivation analyses

The effector, reporter, and reference constructs were co-transfected into *Arabidopsis* leaf protoplasts (Yoo et al. 2007). After 16 h of incubation, protoplasts were lysed and the supernatants assayed for FLUC and RLUC activities with the Dual-Luciferase Reporter Assay System (Promega, Madison, WI, USA). FLUC activity was normalized against RLUC activity in each transfection.

RT-PCR and qRT-PCR analyses

Total RNA was isolated using a plant RNA kit (Omega, Norcross, GA, USA) according to the manufacturer's protocol. Then, 1 μg total RNA was purified from DNA and reverse transcribed into first strand cDNA with the PrimerScript RT Reagent Kit with gDNA Eraser (Takara, Kyoto, Japan) according to the manufacturer's protocol. RT-PCR was conducted with first-strand cDNA as the template. The qRT-PCR was performed with the SYBR Premix Ex Taq Ⅱ (Takara) on LightCycler480 Real-Time PCR System (Roche, Basel, Switzerland). All primers for RT-PCR and qRT-PCR were shown in Tables S2 and S3. The expression level of each gene was normalized to *PP2AA3* according to the comparative ΔΔCT method.

ELISA

The lower inflorescence stems of 7-week-old plants were harvested. Alcohol-insoluble residues (AIR) were prepared by extracting the samples with 96% (v) ethanol at 70°C for 30 min and then air dried (Pettolino et al. 2012). A total of 5 mg dry AIR was treated overnight with 1 mL 1 M KOH at room

temperature. The supernatant was neutralized with acetic acid. A total of 50 µL neutralized solution was applied to 96-well plates (Costar 3590, Corning, NewYork, USA) and dried to the well surfaces by evaporation overnight at 37°C. The plates were blocked with 200 µL of 1% (w/v) instant non-fat dry milk in wash buffer (50 mM Tris-HCl, pH 7.6, containing 100 mM sodium chloride) for 1 h. Blocking agent was removed by aspiration, and 50 µL solution of LM10 or LM11 monoclonal antibodies from rat (Plant Probes, Leeds, UK) were added to each well and incubated for 1 h at room temperature. Supernatant was removed and wells were washed (3x) with 300 µL of 0.1% (w/v) instant non-fat dry milk in wash buffer. Peroxidase-conjugated goat anti-rat IgG (Sigma, San Francisco, CA, USA) was diluted 1:5,000 in wash buffer, and 50 µL was added to each well and incubated for 1 h. Wells were then washed (5x) with 300 µL of wash buffer. The 3,3′,5,5′-tetramethylbenzidine substrate solution was freshly prepared and 100 µL was added to each well. After 20 min, the reaction was stopped by adding 100 µL of 2 M sulfuric acid to each well. The absorbance of each well was measured at 450 nm using a model 680 microplate reader (BIO-RAD, Hercules, CA, USA).

Determination of non-cellulosic monosaccharide composition

AIR from the lower inflorescence stems of the 7-week-old plants was prepared. The non-cellulosic monosaccharide composition of the AIR was analyzed, as previously described (Ebert et al. 2015; **Mélida et al. 2015**).

Glycosyl linkage analysis

Glycosyl linkage composition was performed on the AIR, as described by Pettolino et al. (2012) on a Hewlett-Packard 6890 gas chromatograph with a Hewlett-Packard 5973 mass spectrometer (Agilent) equipped with a BPX 70 column (25 m × 0.22 mm inner diameter, film = 0.25 µm, SGE).

NMR spectroscopy

AIR was suspended in 4 M KOH containing 1% (w/v) $NaBH_4$ and stirred at room temperature for 24 h. The suspensions were passed through a glass-fiber filter, and the filtrates were acidified to pH 5 with glacial acetic acid, extensively dialyzed (3,500 Mr cutoff tubing) against running deionized water, and lyophilized. The dry powders were dissolved with ddH_2O and degraded by β-endoxylanase. Purified xylan oligosaccharides were dissolved in 0.6 mL D_2O (99.9%) and transferred to a 5 mm NMR tube. NMR spectra were recorded at 298 K with an Inova-600 MHz NMR spectrometer. Chemical shifts were measured relative to the internal standard acetone at δ 2.225. Two-dimensional gCOSY, HSQC and HMBC spectra were recorded using standard pulse sequences provided by Varian.

Microscopy

Stem fragments (1 cm) from the bottom of the inflorescence stems were fixed in 3% agarose, before 40-μm thick sections were cut with a microtome and stained with 0.05% toluidine blue for light microscopy. The cell wall thickness of at least 100 cells was measured in light micrograph images.

EMSA

The carboxy-terminal 82 amino acids of KNAT7 containing the homeodomain were fused in-frame with GST and expressed in *Escherichia coli*. The recombinant GST-KNAT7 protein and GST protein were purified using Glutathione Sepharose 4 Fast Flow (GE Healthcare, Little Chalfont, UK). The 3′ end biotin-labeled *IRX9* promotor fragments were incubated with 5 μg of either KNAT7-GST or GST protein in the binding buffer (50 mM Tris-HCl, pH 8.0, 150 mM KCl, 1 mM dithiothreitol (DTT), 1 mM ethylene diaminetetraacetic acid (EDTA)) for 30 min. For competition analyses, unlabeled promoter fragments were included in the binding reactions in either 15 or 30 fold molar excess relative to the labeled probes. Polyacrylamide gel electrophoresis was used to separate the KNAT7-bound and unbound DNA probes and then the DNA were electro-blotted onto a nylon membrane and detected using the chemiluminescent method.

Pyrolysis GC/MS

Milled lower inflorescence stems (1.5 mg) of 7-week-old plants were pyrolysed in an EGA/PY-3030D pyrolyzer (Frontier Laboratories, Saikon Koriyama, Japan) connected to a QP2010 GC/MS system (Shimadzu, Kyoto, Japan) with a DB-5 capillary column (30 mm × 0.25 mm × 0.25 μm, Agilent, Santa Clara, CA, USA). The pyrolysis was initially set at 200°C and held for 1 min, then increased to 600°C at 20°C min^{-1} and held for 10 sec. The GC temperature was started at 40°C and held for 2 min, then increased to 280°C at 5°C min^{-1} and held for 10 min. The carrier gas was helium with a flow of 2 mL min^{-1}. The mass spectra of each compound were identified according to the Wiley and National Institute of Standards and Technology (NIST) libraries. Peak molar areas were calculated for each compound (by dividing the peak area by the respective molecular weights) and the total molar areas were normalized.

ACKNOWLEDGEMENTS

We thank Professor Tsuyoshi Nakagawa (Shimane University, Japan) for providing the pUGW2, pUGW35 and pUGW2-*RLUC* vectors. Financial support for this work was obtained from the National Key Research and Development Program of China (2016YFD0600105), the National Natural Science Foundation of China (31670670, 31670601), the open Foundation (491170K201703) of Provincial Key Laboratory of Agrobiology (Jiangsu Academy of Agricultural Sciences), and the Guangdong Province Science and Technology Projects (2015A050502045). W. Z., C. T. B., and A. B. acknowledge support of a grant from the Australia Research Council (ARC) to the ARC Centre of Excellence in Plant Cell Walls (CE110001007).

AUTHOR CONTRIBUTIONS

A.-M. W. and J.-B. H. designed the study. J.-B. H., X.-H. Z., P.-Z. D., Y.-Q. W., and H.-L., L. performed

the experiments. W. Z., C. T. B., and A. B. carried out the linkage analysis and A.B. contributed to the writing. J.-B. H and A.-M. W. analyzed the data and wrote the manuscript.

REFERENCES

Andersson SI, Samuelson O, Ishihara M, Shimizu K (1983) Structure of the reducing end-groups in spruce xylan. Carbohyd Res 11: 283-288

Bhargava A, Ahad A, Wang S, Mansfield SD, Haughn GW, Douglas CJ, Ellis BE (2013) The interacting MYB75 and KNAT7 transcription factors modulate secondary cell wall deposition both in stems and seed coat in Arabidopsis. Planta 237: 1199-1211

Boerjan W, Ralph J, Baucher M (2003) Lignin biosynthesis. Annu Rev Plant Biol 54: 519-546

Bromley JR, Busse-Wicher M, Tryfona T, Mortimer JC, Zhang Z, Brown DM, Dupree P (2013) GUX1 and GUX2 glucuronyltransferases decorate distinct domains of glucuronoxylan with different substitution patterns. Plant J 74: 423-434

Brown D, Wightman R, Zhang Z, Gomez LD, Atanassov I, Bukowski J, Tryfona T, McQueen-Mason SJ, Dupree P, Turner S (2011) Arabidopsis genes IRREGULAR XYLEM (IRX15) and IRX15L encode DUF579-containing proteins that are essential for normal xylan deposition in the secondary cell wall. Plant J 66: 401-413

Brown DM, Goubet F, Wong VW, Goodacre R, Stephens E, Dupree P, Turner SR (2007) Comparison of five xylan synthesis mutants reveals new insight into the mechanisms of xylan synthesis. Plant J 52: 1154-1168

Brown DM, Zeef LA, Ellis J, Goodacre R, Turner SR (2005) Identification of novel genes in Arabidopsis involved in secondary cell wall formation using expression profiling and reverse genetics. Plant Cell 17: 2281-2295

Brown DM, Zhang Z, Stephens E, Dupree P, Turner SR (2009) Characterization of IRX10 and

IRX10-like reveals an essential role in glucuronoxylan biosynthesis in Arabidopsis. Plant J 57: 732-746

Cassan-Wang H, Goue N, Saidi MN, Legay S, Sivadon P, Goffner D, Grima-Pettenati J (2013) Identification of novel transcription factors regulating secondary cell wall formation in Arabidopsis. Front Plant Sci 4: 189

Clough SJ, Bent AF (1998) Floral dip: A simplified method for Agrobacterium-mediated transformation of Arabidopsis thaliana. Plant J 16: 735-743

del Pozo JC, Boniotti MB, Gutierrez C(2002) Arabidopsis E2Fc functions in celldivision and is degraded by the ubiquitin-SCFAtSKP2 pathway in response to light. Plant Cell 14: 3057–3071

delPozo JC, Diaz-Trivino S,Cisneros N, Gutierrez C (2006) The balance between celldivision and endoreplication depends on E2FC-DPB, transcription factorsregulated by the ubiquitin-SCFSKP2A pathway in Arabidopsis. Plant Cell 18: 2224–2235

Ebert B, Rautengarten C, Guo X, Xiong G, Stonebloom S, Smith-Moritz AM, Herter T, Chan LJG, Adams PD, Petzold CJ, Pauly M, Willats WGT, Heazlewood JL, Scheller HV (2015) Identification and characterization of a golgi-localized UDP-xylose transporter family from Arabidopsis. Plant Cell 27: 1218-1227

Ehlting J, Mattheus N, Aeschliman DS, Li E, Hamberger B, Cullis IF, Zhuang J, Kaneda M, Mansfield SD, Samuels L, Ritland K, Ellis BE, Bohlmann J, Douglas CJ (2005) Global transcript profiling of primary stems from Arabidopsis thaliana identifies candidate genes for missing links in lignin biosynthesis and transcriptional regulators of fiber differentiation. Plant J 42: 618-640

Gong SY, Huang GQ, Sun X, Qin LX, Li Y, Zhou L, Li XB (2014) Cotton KNL1, encoding a class II KNOX transcription factor, is involved in regulation of fibre development. J Exp Bot 65: 4133-4147

Hatton D, Sablowski R, Yung MH, Smith C, Schuch W, Bevan M (1995) Two classes of cis sequences contribute to tissue-specific expression of a PAL2 promoter in transgenic tobacco.

Plant J 7: 859-876

Jensen JK, Johnson NR, Wilkerson CG (2014) Arabidopsis thaliana IRX10 and two related proteins from psyllium and Physcomitrella patens are xylan xylosyltransferases. Plant J 80: 207-215

Jensen JK, Kim H, Cocuron J, Orler R, Ralph J, Wilkerson CG (2011) The DUF579 domain containing proteins IRX15 and IRX15-L affect xylan synthesis in Arabidopsis. Plant J 66: 387-400

Johansson MH, Samuelson O (1977) Reducing end groups in birch xylan and their alkaline degradation. Wood Sci Technol 11: 251-263

Ko JH, Kim WC, Han KH (2009) Ectopic expression of MYB46 identifies transcriptional regulatory genes involved in secondary wall biosynthesis in Arabidopsis. Plant J 60: 649-665

Kuang B, Zhao X, Zhou C, Zeng W, Ren J, Ebert B, Beahan CT, Deng X, Zeng Q, Zhou G, Doblin M, Heazlewood JL, Bacic A, Chen X, Wu AM (2016) Role of UDP-glucuronic acid decarboxylase in xylan biosynthesis in Arabidopsis. Mol Plant 9, 1119–1131.

Kubo M, Udagawa M, Nishikubo N, Horiguchi G, Yamaguchi M, Ito J, Mimura T, Fukuda H, Demura T (2005) Transcription switches for protoxylem and metaxylem vessel formation. Genes Dev 19: 1855-1860

Lee C, O'Neill MA, Tsumuraya Y, Darvill AG, Ye ZH (2007a) The irregular xylem9 mutant is deficient in xylan xylosyltransferase activity. Plant Cell Physiol 48: 1624-1634

Lee C, Teng Q, Huang W, Zhong R, Ye ZH (2009) The F8H glycosyltransferase is a functional paralog of FRA8 involved in glucuronoxylan biosynthesis in Arabidopsis. Plant Cell Physiol 50: 812-827

Lee C, Teng Q, Zhong R, Ye ZH (2011) The four Arabidopsis REDUCED WALL ACETYLATION genes are expressed in secondary wall-containing cells and required for the acetylation of xylan. Plant Cell Physiol 52: 1289-1301

Lee C, Teng Q, Zhong R, Ye ZH (2012a) Arabidopsis GUX proteins are glucuronyltransferases

responsible for the addition of glucuronic acid side chains onto xylan. Plant Cell Physiol 53: 1204-1216

Lee C, Teng Q, Zhong R, Yuan Y, Haghighat M, Ye ZH (2012b) Three Arabidopsis DUF579 domain-containing GXM proteins are methyltransferases catalyzing 4-O-methylation of glucuronic acid on xylan. Plant Cell Physiol 53: 1934-1949

Lee C, Zhong R, Richardson EA, Himmelsbach DS, McPhail BT, Ye ZH (2007b) The PARVUS gene is expressed in cells undergoing secondary wall thickening and is essential for glucuronoxylan biosynthesis. Plant Cell Physiol 48: 1659-1672

Lee C, Zhong R, Ye ZH (2012c) Arabidopsis family GT43 members are xylan xylosyltransferases required for the elongation of the xylan backbone. Plant Cell Physiol 53: 135-143

Li E, Bhargava A, Qiang W, Friedmann MC, Forneris N, Savidge RA, Johnson LA, Mansfield SD, Ellis BE, Douglas CJ (2012) The Class II KNOX gene KNAT7 negatively regulates secondary wall formation in Arabidopsis and is functionally conserved in Populus. New Phytol 194: 102-115

Li E, Wang S, Liu Y, Chen J, Douglas CJ (2011) OVATE FAMILY PROTEIN4 (OFP4) interaction with KNAT7 regulates secondary cell wall formation in Arabidopsis thaliana. Plant J 67: 328-341

Liu Y, You S, Taylor-Teeples M, Li WL, Schuetz M, Brady SM, Douglas CJ (2014) BEL1-LIKE HOMEODOMAIN6 and KNOTTED ARABIDOPSIS THALIANA7 interact and regulate secondary cell wall formation via repression of REVOLUTA. Plant Cell 26: 4843-4861

McCarthy RL, Zhong R, Ye ZH (2009) MYB83 is a direct target of SND1 and acts redundantly with MYB46 in the regulation of secondary cell wall biosynthesis in Arabidopsis. Plant Cell Physiol 50: 1950-1964

McCartney L, Marcus SE, Knox JP (2005) Monoclonal antibodies to plant cell wall xylans and arabinoxylans. J Histochem Cytochem 53: 543-546

Mélida H, Largo-Gosens A, Novo-Uzal E, Santiago R, Pomar F, García P, García-Angulo P, Acebes J L, Álvarez J, Encina A (2015) Ectopic lignification in primary cellulose-deficient cell walls of maize cell suspension cultures. J Integr Plant Biol 57: 357–372

Mitsuda N, Iwase A, Yamamoto H, Yoshida M, Seki M, Shinozaki K, Ohme-Takagi M (2007) NAC transcription factors, NST1 and NST3, are key regulators of the formation of secondary walls in woody tissues of Arabidopsis. Plant Cell 19: 270-280

Mortimer JC, Miles GP, Brown DM, Zhang Z, Segura MP, Weimar T, Yu X, Seffen KA, Stephens E, Turner SR, Dupree P (2010) Absence of branches from xylan in Arabidopsis gux mutants reveals potential for simplification of lignocellulosic biomass. Proc Natl Acad Sci USA 107: 17409-17414

Ohtani M, Akiyoshi N, Takenaka Y, Sano R, Demura T (2017) Evolution of plant conducting cells: Perspectives from key regulators of vascular cell differentiation. J Exp Bot 68: 17-26

Pandey SK, Nookaraju A, Fujino T, Pattathil S, Joshi CP (2016) Virus-induced gene silencing (VIGS)-mediated functional characterization of two genes involved in lignocellulosic secondary cell wall formation. Plant Cell Rep 35:2353-2367

Pauly M, Gille S, Liu L, Mansoori N, Souza DA, Schultink A, Xiong G (2013) Hemicellulose biosynthesis. Planta 238: 627-642

Peña MJ, Zhong R, Zhou GK, Richardson EA, O'Neill MA, Darvill AG, York WS, Ye ZH (2007) Arabidopsis irregular xylem8 and irregular xylem9: Implications for the complexity of glucuronoxylan biosynthesis. Plant Cell 19: 549-563

Pettolino FA, WalshC, FincherGB, Bacic A (2012) Determining the polysaccharide composition of plant cell walls. Nat Protoc 7: 1590–1607

Romano JM, Dubos C, Prouse MB, Wilkins O, Hong H, Poole M, Kang KY, Li E, Douglas CJ, Western TL, Mansfield SD, Campbell MM (2012) AtMYB61, an R2R3-MYB transcription factor, functions as a pleiotropic regulator via a small gene network. New Phytol 195: 774-786

Scheible WR, Pauly M (2004) Glycosyltransferases and cell wall biosynthesis: Novel players and insights. Curr Opin Plant Biol 7: 285-295

Taylor-Teeples M, Lin L,de LucasM,Turco G,Toal TW, Gaudinier A, Young NF, Trabucco GM, Veling MT, LamotheR, HandakumburaPP, Xiong G, Wang C, Corwin J, Tsoukalas A, Zhang L, Ware D, Pauly M, Kliebenstein DJ, Dehesh K, Tagkopoulos I, Breton G, Pruneda-Paz JL, Ahnert SE, Kay SA, Hazen SP, Brady SM (2015) An Arabidopsis gene regulatory network for secondary cell wall synthesis. Nature 517: 571–575

Urbanowicz BR, Peña MJ, Moniz HA, Moremen KW, York WS (2014) Two Arabidopsis proteins synthesize acetylated xylan in vitro. Plant J 80: 197-206

Urbanowicz BR, Pena MJ, Ratnaparkhe S, Avci U, Backe J, Steet HF, Foston M, Li H, O'Neill MA, Ragauskas AJ, Darvill AG, Wyman C, Gilbert HJ, York WS (2012) 4-O-methylation of glucuronic acid in Arabidopsis glucuronoxylan is catalyzed by a domain of unknown function family 579 protein. Proc Natl Acad Sci USA 109: 14253-14258

Walhout AJ, Temple GF, Brasch MA, Hartley JL, Lorson MA, van den Heuvel S, Vidal M (2000) GATEWAY recombinational cloning: Application to the cloning of large numbers of open reading frames or ORFeomes. Methods Enzymol 328: 575-592

Wu AM, Rihouey C, Seveno M, Hörnblad E, Singh SK, Matsunaga T, Ishii T, Lerouge P, Marchant A (2009) The Arabidopsis IRX10 and IRX10-LIKE glycosyltransferases are critical for glucuronoxylan biosynthesis during secondary cell wall formation. Plant J 57: 718-731

Wu AM, Hornblad E, Voxeur A, Gerber L, Rihouey C, Lerouge P, Marchant A (2010) Analysis of the Arabidopsis IRX9/IRX9-L and IRX14/IRX14-L pairs of glycosyltransferase genes reveals critical contributions to biosynthesis of the hemicellulose glucuronoxylan. Plant Physiol 153: 542-554

Xiong G, Cheng K, Pauly M (2013) Xylan O-acetylation impacts xylem development and enzymatic recalcitrance as indicated by the Arabidopsis mutant tbl29. Mol Plant 6: 1373-1375

Yamaguchi M, Kubo M, Fukuda H, Demura T (2008) Vascular-related NAC-DOMAIN7 is involved in the differentiation of all types of xylem vessels in Arabidopsis roots and shoots. Plant J 55: 652-664

Yoo SD, Cho YH, Sheen J (2007) Arabidopsis mesophyll protoplasts: A versatile cell system for transient gene expression analysis. Nat Protoc 2: 1565-1572

Yuan Y, Teng Q, Zhong R, Ye ZH (2013) The Arabidopsis DUF231 domain-containing protein ESK1 mediates 2-O- and 3-O-acetylation of xylosyl residues in xylan. Plant Cell Physiol 54: 1186-1199

Zhao X, Liu N, Shang N, Zeng W, Ebert B, Rautengarten C, Zeng QY, Li H, Chen X, Beahan C, Bacic A, Heazlewood J, Wu AM (2017) Three UDP-xylose transporters (UXTs) participate in xylan biosynthesis by conveying cytosolic UDP-xylose into the Golgi lumen in *Arabidopsis*. J Exp Bot 69, doi.org/10.1093/jxb/erx448

Zhang B, Zhou Y (2011) Rice Brittleness Mutants: A Way to Open the 'Black Box' of Monocot Cell Wall Biosynthesis. J Integr Plant Biol 53: 136-142.

Zeng W, Lampugnani ER, Picard KL, Song L, Wu AM, Farion IM, Zhao J, Ford K, Doblin MS, Bacic A (2016) Asparagus IRX9, IRX10, and IRX14A are components of an active xylan backbone synthase complex that forms in the golgi apparatus. Plant Physiol 171: 93-109

Zhong R, Demura T, Ye ZH (2006) SND1, a NAC domain transcription factor, is a key regulator of secondary wall synthesis in fibers of *Arabidopsis*. Plant Cell 18: 3158-3170

Zhong R, Lee C, Ye ZH (2010a) Evolutionary conservation of the transcriptional network regulating secondary cell wall biosynthesis. Trends Plant Sci 15: 625-632

Zhong R, Lee C, Ye ZH (2010b) Global analysis of direct targets of secondary wall NAC master switches in *Arabidopsis*. Mol Plant 3: 1087-1103

Zhong R, Lee C, Zhou J, McCarthy RL, Ye ZH (2008) A battery of transcription factors involved in the regulation of secondary cell wall biosynthesis in *Arabidopsis*. Plant Cell 20: 2763-2782

Zhong R, Richardson EA, Ye ZH (2007) The MYB46 transcription factor is a direct target of SND1 and regulates secondary wall biosynthesis in *Arabidopsis*. Plant Cell 19: 2776-2792

Zhong R, Ye Z (2015) The *Arabidopsis* NAC transcription factor NST2 functions together with SND1 and NST1 to regulate secondary wall biosynthesis in fibers of inflorescence stems. Plant Signal Behav 10: e989746

Zhong R, Ye ZH (1999) *IFL1*, a gene regulating interfascicular fiber differentiation in *Arabidopsis*, encodes a homeodomain-leucine zipper protein. Plant Cell 11: 2139-2152

Zhong R, Ye ZH (2012) MYB46 and MYB83 bind to the SMRE sites and directly activate a suite of transcription factors and secondary wall biosynthetic genes. Plant Cell Physiol 53: 368-380

Zhong R, Ye ZH (2014) Secondary cell walls: Biosynthesis, patterned deposition and transcriptional regulation. Plant Cell Physiol 56: 195-214

Zhou J, Zhong R, Ye ZH (2014) *Arabidopsis* NAC domain proteins, VND1 to VND5, are transcriptional regulators of secondary wall biosynthesis in vessels. PLoS ONE 9: e105726

Zuo J, Niu QW, Chua NH (2000) An estrogen receptor-based transactivator XVE mediates highly inducible gene expression in transgenic plants. Plant J 24: 265-273

SUPPORTING INFORMATION

Figure S1. MYB46 activates the promoters of xylan biosynthetic genes

Transactivation analyses showing the effects of MYB46 on the induction of the *FLUC* reporter gene driven by the promoters of *IRX9*, *IRX9-L*, *IRX10*, *IRX10-L*, *IRX14*, *IRX14-L*, *FRA8*, or *F8H*. The FLUC relative activity in protoplasts transfected with no effector construct was used as a control and set to one. Mean and standard error (*SE*) were from three biological replicates. Values significantly different from the controls are marked with asterisks ($^{*}P < 0.05$ and $^{**}P < 0.01$; *t*-test).

Figure S2. Analysis of lignin content in WT and *knat7* plants

Lignin content from the lower half of inflorescence stems taken from 7-week-old plants. Data are mean and SE from three biological replicates ($^{*}P < 0.05$; *t*-test).

Table S1. Primer sequences for cloning genes and promotors

Table S2. Primer sequences for RT-PCR

Table S3. Primer sequences for qRT-PCR

Figure legends:

Figure 1. KNAT7 activates the promoters of the major xylan biosynthetic genes

(A) Diagrams of the effector, reporter, and reference constructs used for the transactivation analyses. The effector constructs contain the coding sequences of the TF driven by the CaMV*35S* promoter. The reporter constructs consist of the *FLUC* reporter gene driven by the promoters of the *IRX9*, *IRX9L*, *IRX10*, *IRX10L*, *IRX14*, *IRX14L*, *FRA8*, and *F8H* genes. The reference construct contains the *RLUC* reporter gene driven by the CaMV*35S* promoter. **(B)** Transactivation analyses showing the effects of KNAT7 on the induction of the *FLUC* reporter gene driven by the promoters of *IRX9*, *IRX9L*, *IRX10*, *IRX10L*, *IRX14*, *IRX14L*, *FRA8*, and *F8H* genes. The FLUC relative activity in protoplasts transfected with no effector construct was used as a control and set to one. Mean and SE were from three biological replicates. Values significantly different from the controls are marked with asterisks ($^{*}P < 0.05$ and $^{**}P < 0.01$; *t*-test).

Figure 2. Cell wall sugar analyses of *knat7* mutant and WT plants

(A) RT-PCR analysis of *KNAT7* expression in WT and *knat7* plants. *ACTIN 2* (*ACT2*) was used as a positive control. **(B)** Relative abundance of xylan epitopes detected by ELISA. Mean and SE were from three biological replicates. **(C)** Non-cellulosic monosaccharide composition of total cell wall extracts. Each sample consisted of 20 pooled individuals and data represented mean and SE of five technical replicates. Values expressed in mol%. GalA, galacturonic acid. **(D)** Partial 600-MHz ^{1}H NMR spectra of acidic xylo-oligosaccharides generated by β-endoxylanase digestion of the 4 M KOH-soluble fractions from the stems of WT and *knat7* plants. For all data, values significantly different from WT plants are marked with asterisks ($^{*}P < 0.05$ and $^{**}P < 0.01$; *t*-test).

Figure 3. Effects of *KNAT7* loss-of-function and overexpression on secondary wall thickening

(A, B) RT-PCR analysis of *KNAT7* expression in WT, *KNAT7*-OE and *35S*: *KNAT7*/*knat7* plants.

ACT2 was used as a positive control. The numbers refer to different transformed lines. **(C)** The vascular bundles (up) and interfascicular fibers (down) of WT, *knat7*, *KNAT7*-OE and *35S*: *KNAT7*/*knat7* plants. Stem cross sections were taken from the bases of the inflorescence stems of 6-week-old plants and stained with toluidine blue. Bars = 30 μm.

Figure 4. qRT-PCR expression profiling of xylan biosynthetic genes in *knat7* mutants and *KNAT7*-OE plants

(A) Expression of xylan biosynthetic genes in lower inflorescence stems of *knat7* mutants relative to WT plants. **(B)** Expression of xylan biosynthetic genes in lower inflorescence stems of *KNAT7*-OE plants relative to WT. The expression level of each gene in the WT plant was set to unity. *PROTEIN PHOSPHATASE 2A SUBUNIT A3* (*PP2AA3*) was used as the reference gene. Each sample consisted of pooled stems from 8–10 plants. Mean and SE were from three biological replicates. Values significantly different from the WT plants are marked with asterisks ($^{*}P < 0.05$ and $^{**}P < 0.01$; *t*-test).

Figure 5. KNAT7 binds to the *IRX9* promoter

(A) Transactivation analyses showing KNAT7-activated expression of the *FLUC* reporter gene driven by the corresponding *IRX9* promoter deletions. The left panel illustrates various deletions of the *IRX9* promoter (−1,506 to −1bp from the start codon). FLUC relative activity in protoplasts transfected with no effector construct was used as a control and set to one. Mean and SE were from three biological replicates. Values significantly different from the controls are marked with asterisks ($^{*}P < 0.05$ and $^{**}P < 0.01$, *t*-test). **(B)** EMSA of KNAT7 binding to the biotin-labeled −209 to −157 bp and −169 to −117 bp fragments of the *IRX9* promoter. The faint band (marked with an asterisk) above the probe is non-specific product. **(C)** EMSA of KNAT7 binding to a 53 bp fragment (located between −236 and −184 bp relative to the start codon) of the *IRX9* promoter. The position of the binding band is labeled with an arrow. For competition analyses, unlabeled DNA fragments (competitors) in either 15-fold (+)

or 30-fold (++) molar excess, relative to the labeled probes, were included in the reactions. GST was used as a control protein.

Figure 6. Model for the role of KNAT7 in the regulation of xylan biosynthesis

VND6, VND7, SND1, NST1, and NST2 are the master regulators of secondary wall biosynthesis. MYB46 and MYB83 act as second-level master regulators. IRX9, IRX9L, IRX10, IRX10L, IRX14 and IRX14L are involved in xylan backbone extension, whereas FRA8, F8H, IRX8, and PARVUS are associated with biosynthesis of the xylan reducing end. Solid arrows represent direct transcriptional activation and dotted arrows represent transcriptional activation that has not been demonstrated to be direct.

Table 1. Glycosyl linkage composition (mol%) in the AIR fractions of WT and *knat7 Arabidopsis* stems

Glycosyl linkage	WT	*knat7*
Total Cellulose	**47.53**	**50.9**
1,4-Glc	47.53	50.9
Total heteroxylan	**25.4**	**21.04**
1,4-Xyl (p)	18.2	15.8
1,2,4-Xyl (p)	1.43	1.03
1,3,4-Xyl (p)	0.67	0.3
1,2,3,4-Xyl (p)	5.1	3.9
Total heteromannan	**7.1**	**7.27**
1,4-Man (p)	2.57	2.7
1,4,6-Man (p)	0.5	0.47
1,4-Glc (p)	2.57	2.70
1,4,6-Glc (p)	0.5	0.47
t-Gal	0.97	0.93
Total xyloglucan	**11.03**	**11.2**
1,4,6-Glc (p)	2.30	2.33
1,4-Glc (p)	2.3	2.33
1,2-Xyl (p)	2.03	1.77
1,2-Gal (p)	1.6	1.57
t-Fuc (p)	0.3	0.5
t-Xyl	2.5	2.7
Total callose	**0.07**	**0.3**
1,3-Glc (p)	0.07	0.30
Total arabinan	**1.83**	**2.03**
1,5-Ara (f)	1.63	1.73
1,2,5-Ara (f)	0.2	0.3
Total type I AG	**1.63**	**1.33**
1,4-Gal (p)	1.63	1.33
Total type II AG	**0.67**	**0.73**
1,6-Gal (p)	0.3	0.3
1,2-Ara (f)	0.2	0.17
1,3,6-Gal (p)	0.17	0.27
Total RG I/II	**0.13**	**0.07**

1,2-Rha (p)	0.03	0
1,2,4-Rha (p)	0.09	0.07
Total	**95.26**	**94.87**

Each dataset represents the mean of three biological replicates, each performed in duplicate (technical replicates). Glc, glucose; Ara, arabinose; Man, mannose; Gal, galactose; Fuc, fucose; Rha, rhamnose; AG, arabinogalactan; RG, rhamnogalacturonan.

Table 2. Secondary cell wall thickness in the lower inflorescence of 6-week-old WT, *knat7* and *KNAT7*-OE *Arabidopsis* stems

Genotype	Vessel element wall thickness (μm)	Xylary fiber wall thickness (μm)	Interfascicular fiber wall thickness (μm)
WT	1.14 ± 0.18	1.04 ± 0.13	1.29 ± 0.20
knat7	0.91 ± 0.14***	0.89 ± 0.08***	1.64 ± 0.21***
KNAT7-OE	1.24 ± 0.15***	1.13 ± 0.09***	1.12 ± 0.15***

Data are mean ± standard deviation (*SD*) from at least 100 cells measured from light micrographs of the base of inflorescence stems. *** indicates significance (*t*-test) at the $P < 0.001$ level from WT plants.

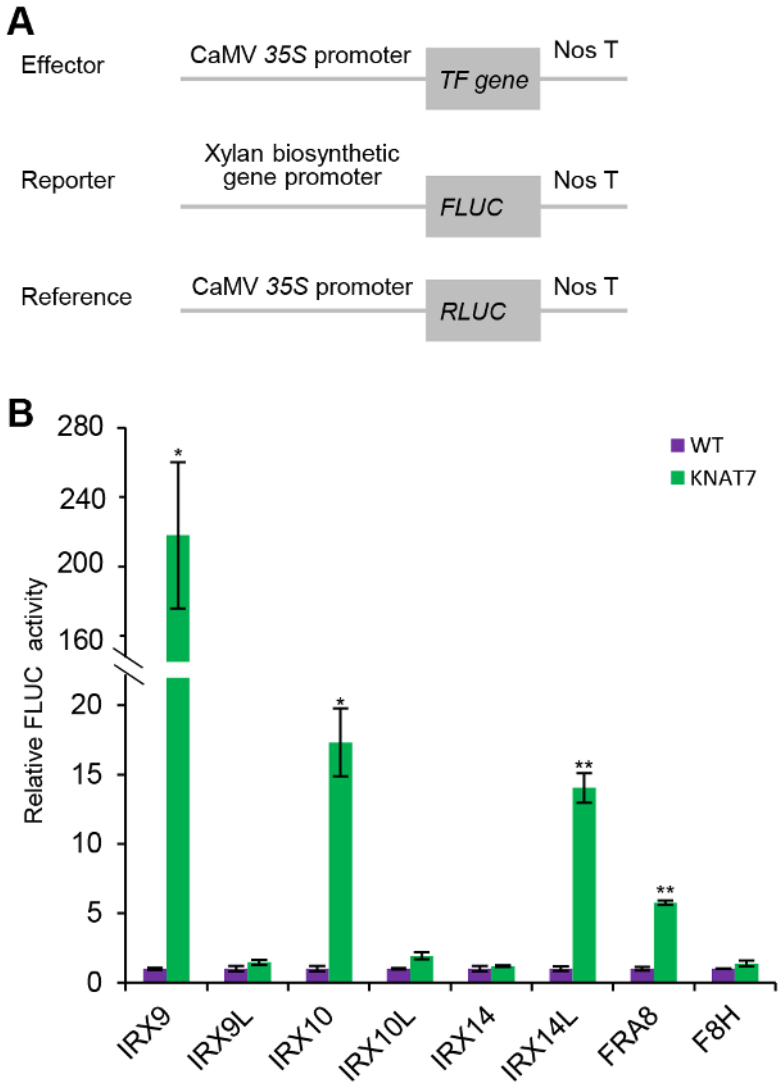

Figure. 1

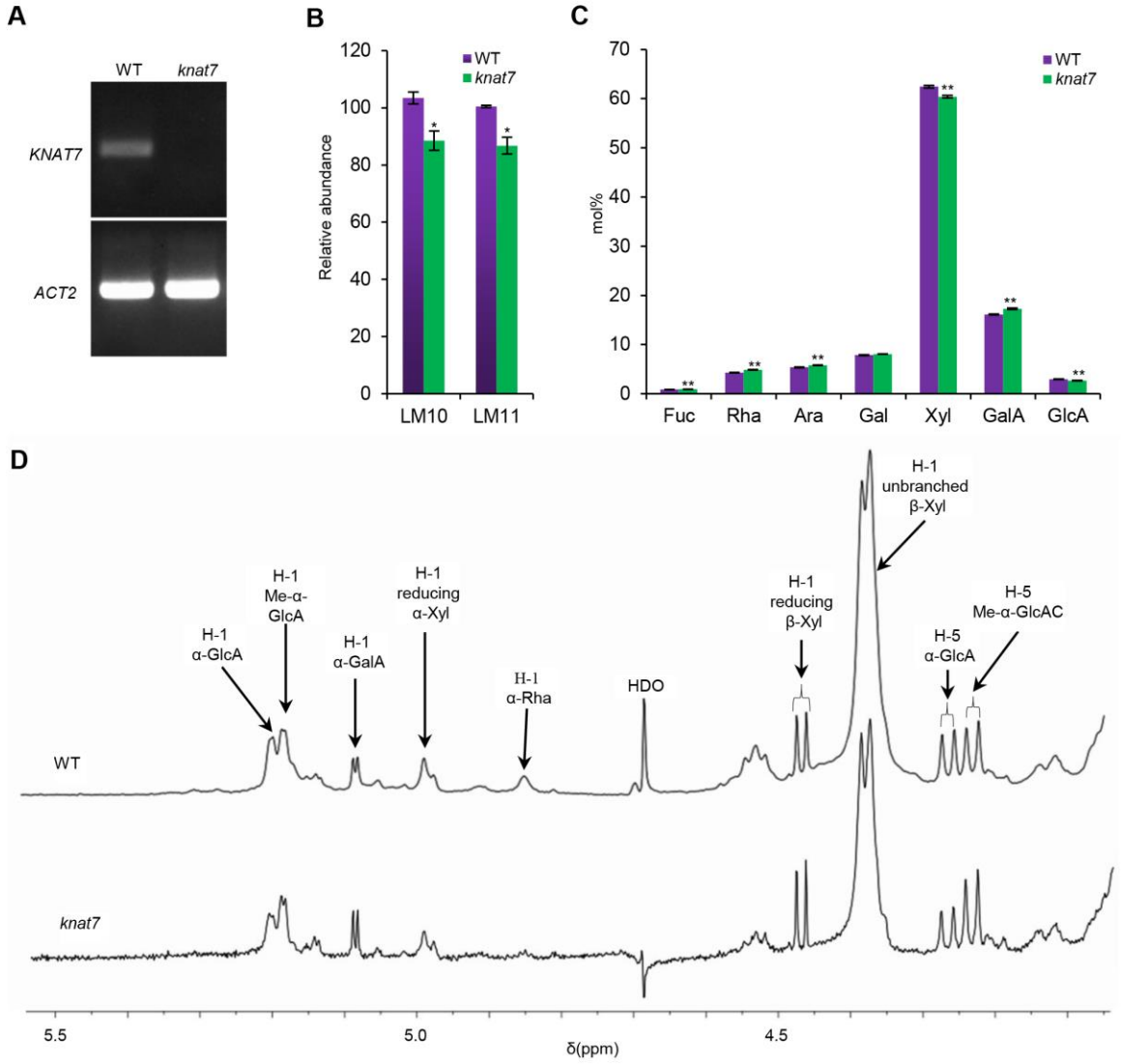

Figure. 2

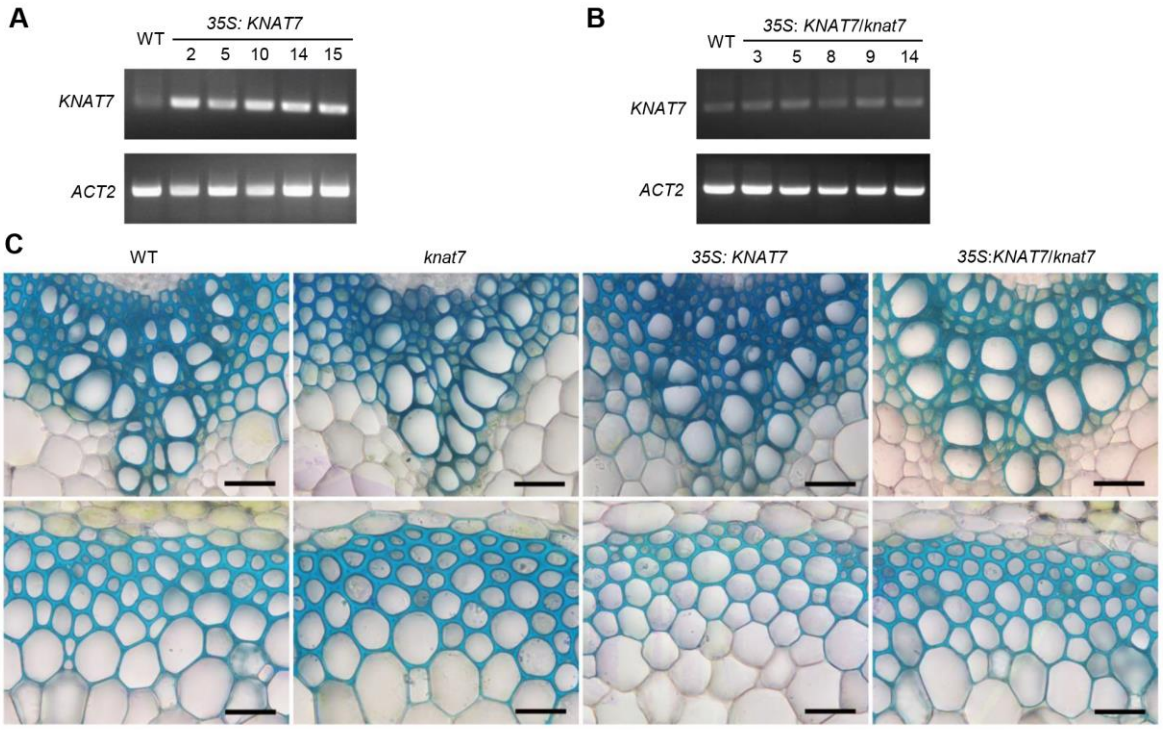

Figure. 3

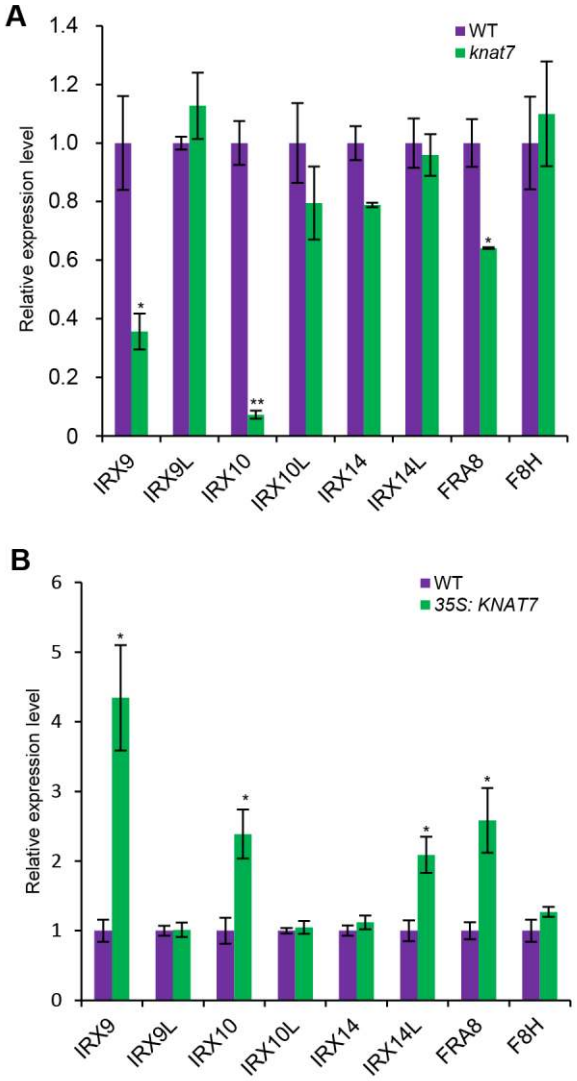

Figure. 4

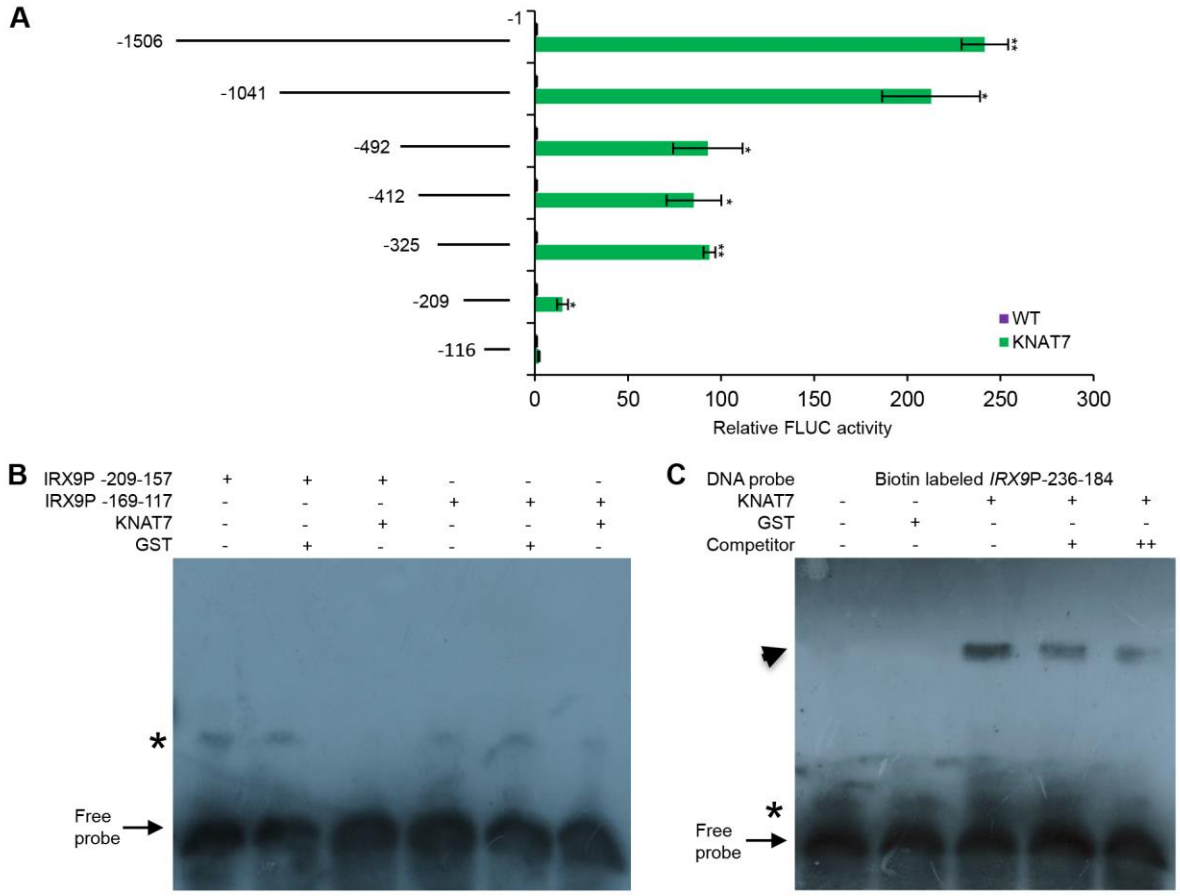

Figure. 5

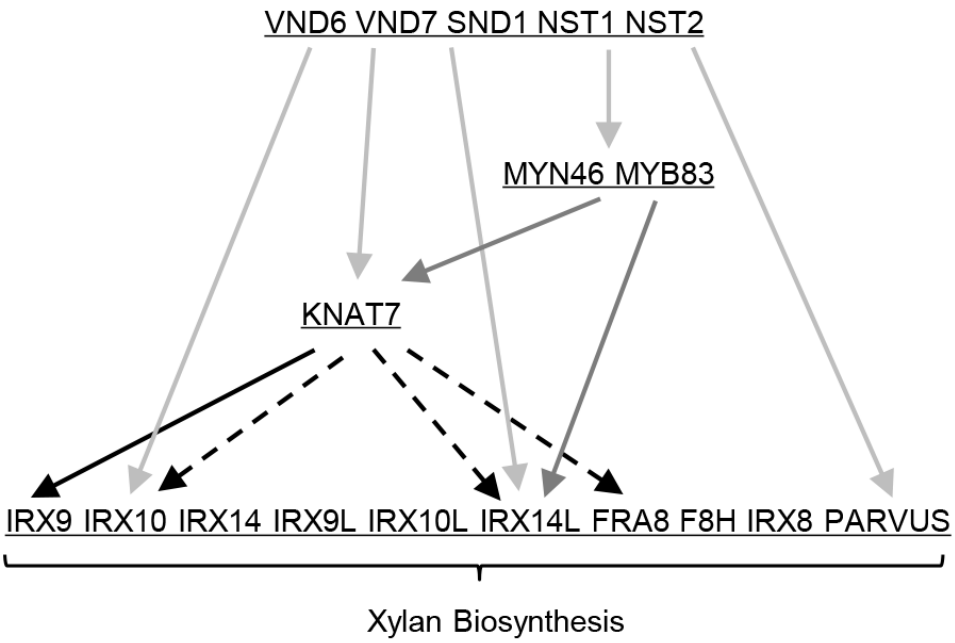

Figure. 6

Author/s:
He, J-B;Zhao, X-H;Du, P-Z;Zeng, W;Beahan, CT;Wang, Y-Q;Li, H-L;Bacic, A;Wu, A-M

Title:
KNAT7 positively regulates xylan biosynthesis by directly activating IRX9 expression in Arabidopsis

Date:
2018-06-01

Citation:
He, J. -B., Zhao, X. -H., Du, P. -Z., Zeng, W., Beahan, C. T., Wang, Y. -Q., Li, H. -L., Bacic, A. & Wu, A. -M. (2018). KNAT7 positively regulates xylan biosynthesis by directly activating IRX9 expression in Arabidopsis. JOURNAL OF INTEGRATIVE PLANT BIOLOGY, 60 (6), pp.514-528. https://doi.org/10.1111/jipb.12638.